1000-nm IR Supercontinuum Due to Raman Soliton Supported by Four-Wave Mixing

Marina Zajnulina
Aston Institute of Photonic Technologies, Aston University, B4 7ET Birmingham, United Kingdom
Author e-mail address: m.zajnulina@aston.ac.uk

Abstract: Simple, low-cost, and robust telecom-fiber-based single-pass system is introduced and numerically studied to generate a supercontinuum ranging from 1500 nm to 2500 nm despite the optical loss due to infrared absorption in optical fibers.

1. Introduction

Infrared spectroscopy is a powerful analytical technique deployed in different fields of technology and science such as chemistry, monitoring of greenhouse gases, food industry, artworks conservation, analysis of polymers and semiconductor microelectronics, and medical diagnostics [1]. In fiber optics, various techniques including passive mode-locking of lasers as well as nonlinear propagation of light in standard and photonic crystal fibers have been introduced in the last two decades to generate supercontinua going from visible range to around $1850\ \mathrm{nm}$ [2,3]. The limitation to further development of the supercontinuum on the red side of the spectrum is set by the infrared absorption in silica fiber that increases almost exponentially for wavelengths beyond $1650\ \mathrm{nm}$ [4]. Here, I introduce and numerically study a simple, low-cost, and robust single-pass fiber system that allows for pushing the supercontinuum spectrum up to 2500 nm despite the action of optical loss. This occurs due to a non-trivial interplay between the noise amplification due to modulational instability (MI) and the growth of a 3rd band Raman seed that arises in the system thanks to a bi-chromatic input provided by two continuous (CW) lasers.

2. Experimental Setup and Model

The single-pass system to generate the supercontinuum consists of three concatenated optical fibers: a standard telecom single-mode fiber (SMF28), an erbium-doped suitably pumped fiber amplifier (EDFA), and a low-dispersion highly nonlinear fiber (HNLF). Two equally intense continuous-wave (CW) lasers producing a modulated cosine-wave at central wavelength of $\lambda_c = 1550\ \mathrm{nm}$ are used to pump the fibers. This central wavelength λ_c is chosen to effectively exploit the amplification of the EDFA that is a standard telecom component. One of the lasers is fixed at the carrier frequency ω_1, the frequency ω_2 of other laser is tunable allowing for adjustment of the spectral laser frequency separation $\mathrm{LFS} = |\,\omega_2 - \omega_1|/2\pi$. More details on the experimental setup and results proving its functionality can be found in the previous related work [5]. The same reference as well as Ref. [6] provide detailed information how the proposed system can be studied using Generalized Nonlinear Schrödinger Equation (GNLS) for the slowly varying optical field. Additionally, I introduce optical loss due to infrared absorption in silica that I model using an exponential function approximating absorption profile of silica fibers (Fig. 1, right, orange). For EDFA, the loss is set to zero. Other system parameters used in the following study are: SMF28: $\beta_2 = -15\ \mathrm{ps^2/km}$, $\beta_3 = 0.1\ \mathrm{ps^3/km}$, $\gamma = 2\ \mathrm{W^{-1}km^{-1}}$, $\mathrm{L} = 350\ \mathrm{m}$; EDFA: $\beta_2 = -1.5\ \mathrm{ps^2/km}$, $\beta_3 = 0.1\ \mathrm{ps^3/km}$, $\gamma = 2\ \mathrm{W^{-1}km^{-1}}$, $\mathrm{L} = 20\ \mathrm{m}$; HNLF: $\beta_2 = -2.5\ \mathrm{ps^2/km}$, $\beta_3 = 0.0081\ \mathrm{ps^3/km}$, $\gamma = 2\ \mathrm{W^{-1}km^{-1}}$, fibre length L is variable.

3. Results

Fig. 1 shows the development of a supercontinuum with a spectral range of $\Delta\lambda \approx 1000\ \mathrm{nm}$. In the SMF28, cascaded four-wave mixing (FWM) started by two initial laser lines yields the development of a frequency comb with line spacing that equals the laser frequency separation $\mathrm{LSF} = 40\ \mathrm{GHz}$ (Fig. 1, right). In the temporal domain, this implies the formation of a soliton crystal with the according component repetition time of $\mathrm{T} = 1/\mathrm{LSF} = 25\mathrm{ps}$ [6]. The soliton order N of the soliton crystal components implies the evolution of higher-order solitons: $\mathrm{N} = \sqrt{\frac{\gamma_{\mathrm{SMF28}} \cdot \mathrm{P_0}}{(2\pi \cdot \mathrm{LSF})^2 |\beta_{2/\mathrm{SMF28}}|}} \approx 2.3$ [7]. In the EDFA, the initial frequency comb gets broadened due to further cascaded FWM and pulse compression based on Erbium amplification (Fig. 1, right) (cf. [8]). After the propagation through the EDFA, the width of the frequency comb is around $500\ \mathrm{GHz}$, the peak power of the soliton crystal components is amplified to several tens of Watts which is sufficient to effectively induce Raman scattering in the HNLF stage.

When the comb from EDFA starts to propagate through the HNLF stage, it starts to build up a spectral pedestal that arises due to modulational instability (MI) amplification of the noise floor (Fig. 2, left, dark-blue) [9]. In the temporal domain, it coincides with a strong pulse compression and distortion. During this process, a Raman seed (RS) arises and gets amplified out of noise at the distance of around $43\ \mathrm{THz}$ from the comb which corresponds to the 3rd Raman band (cf. [9]) (Fig. 2, left, dark-blue).

Fig. 1 Evolution of the supercontinuum in all three fiber stage for input power P_0=2.5 W, laser frequency separation LSF=40 GHz, and HNLF length of L=50 m.

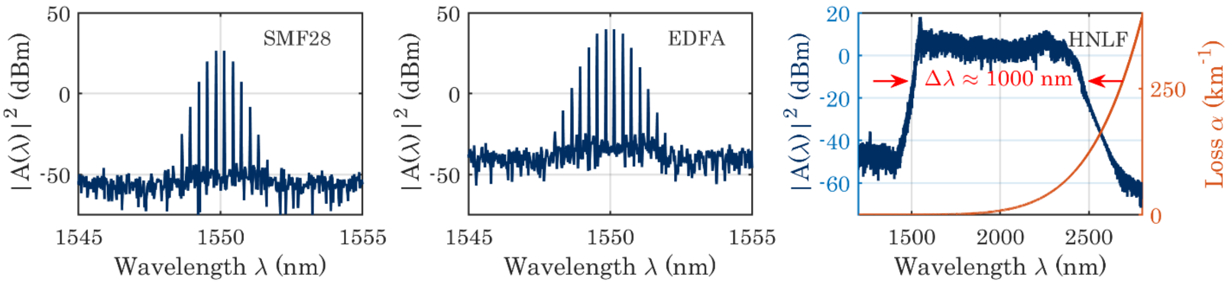

A symmetric anti-Stokes seed (AS) arises with further propagation through the fiber. As the bi-chromatic input further propagates through the HNLF stage, the RS seed continues to grow despite the impact of optical losses until it reaches the Raman threshold and gives rise to a Raman soliton (Fig. 2, right, dark-blue, 20 m) (cf. [9]). The Raman soliton travels to the red side of the spectrum due to the soliton self-frequency shift [3], whereas the noise in the spectral window between the comb and the Raman soliton gets amplified which results in the formation of an broad supercontinuum spectrum with an almost equal spectral intensity.

For comparison, when only a monochromatic sech-profile pulse is used as initial condition (Fig. 2, left, orange), the explanation of the spectral broadening is straight forward: the high nonlinearity in the HNLF induces a growth of a spectral pedestal due to the impact of MI which coincides with pulse compression and distortion in the temporal domain. The spectral broadening provides a seed for Raman amplification on the red side of the spectrum due to intra-pulse Raman scattering. Is the first seed at the distance of 13 THz strong enough, it evolves to a fundamental Raman soliton self-shifted to the red and providing amplification for further Raman spectral bands and the corresponding Raman solitons [3,9]. The resulting cascade of fundamental Raman solitons is clearly seen in the bottom picture of Fig. 2, right. As the pictures on the left side of Fig. 2 show, the spectral intensity that arises due to a cascade or self-shifted Raman solitons is subject to a greater variation than the spectral intensity of the bi-chromatic input. Also, the latter is up to 200 nm broader than its counterpart although both are subject to the same value of optical loss due to infrared absorption in silica. In both cases, the optical loss defines the optimal length L_{HNLF}^{OPT} of the HNLF stage at which the spectral broadening is maximal. Until L_{HNLF}^{OPT} is reached, the spectral broadening keeps evolving. After that, it is counterbalanced by optical loss. In the simulations, the optimal length for a bi-chromatic input is $L_{HNLF}^{OPT} = 35$ m with $\Delta\lambda \approx 1000$ nm.

Fig. 3, left shows the evolution of the supercontinuum range $\Delta\lambda$ (cf. Fig. 1, right) for different values of LFS and input power P_0. The nonlinearity that governs MI and Raman scattering increases with P_0 which leads to the increase of $\Delta\lambda$. The orange points denote the value of LSF at which the broadening of $\Delta\lambda$ occurs via the emission of an independent Raman soliton additionally to the process described above. Apparently, the emission of a Raman soliton occurs with smaller values of LSF if the P_0 decreases. Fig. 3, right shows the dependence of the supercontinuum range $\Delta\lambda$ from input P_0. For low input powers, MI is the only process to drive the spectral brodening. For higher input powers, it occurs due to a common action of MI and Raman soliton. As the orange points show, there is, theoretically, no limitation to the increase of $\Delta\lambda$. Thus, fibers with negligible losses beyond 1600 nm (as, for instance, ZBLAN fibers) have a potential to produce extremely broad supercontinua for NIR range suitable for intfrared spectroscopy.

Fig. 2 Left: Comparison between the evolution of the supercontinuum for a two-laser input with LSF $= 40$ GHz (dark-blue) and a single monochromatic sech-profile pulse (orange) with FWHM of 3.8 ps. The peak power is $P_0 = 2.5$ W and HNLF length $L = 50$ m. Right: Evolution of the supercontinuum spectral range $\Delta\lambda$ along the fiber for the same two-laser (top) and monochromatic sech-pulse (bottom) input.

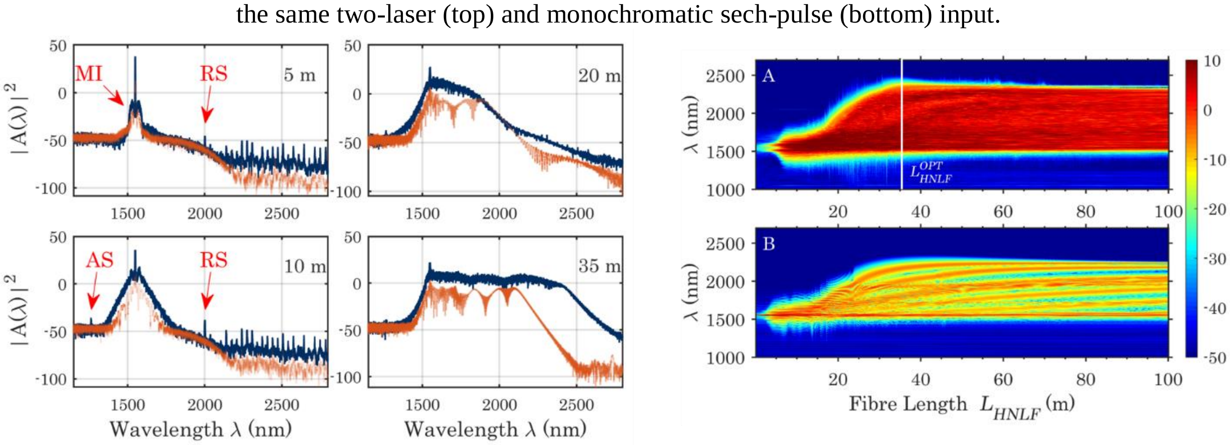

Fig. 3 Left: Evolution of the supercontinuum range $\Delta\lambda$ for different values of laser frequency separation LFS and input power P_0. Right: supercontinuum range $\Delta\lambda$ for LFS $= 40$ GHz and different values of P_0 for included and excluded optical loss. The length of HNLF is $L = 35$ m in both cases.

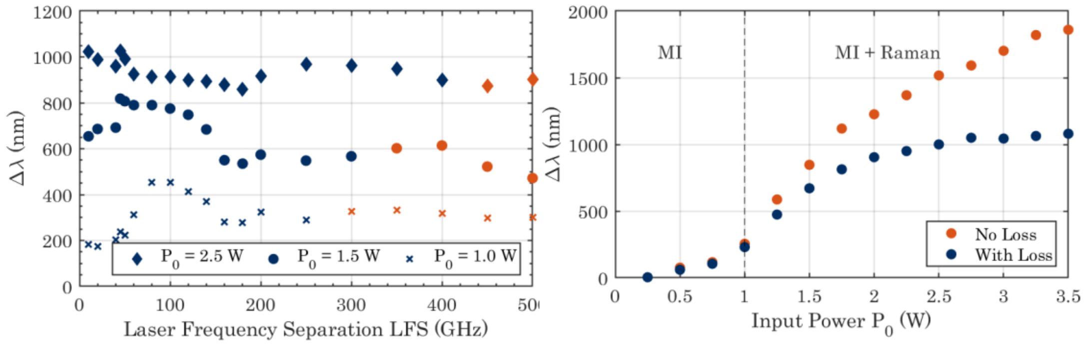

4. Conclusion and Outlook

In this paper, a simple, robust, and low-cost fiber system was introduced and numerically studied that allows for generation of 1000 nm broad supercontinuum ranging from 1500 nm to 2500 nm despite the action of optical loss due to infrared absorption in silica fibers. It consists of three concatenated optical fibers: a standard telecom single-mode fiber (SMF28), an erbium-doped suitably pumped fiber amplifier (EDFA), and a low-dispersion highly nonlinear fiber (HNLF). Two equally intense continuous-wave (CW) lasers producing a modulated cosine-wave at central wavelength of $\lambda_c = 1550$ nm are used to pump the fibers. The supercontinuum arises when the frequency comb formed due to a cascade of four-wave-mixing process in the SMF28, amplified and further broadened in the EDFA propagates trough the HNLF stage. Here is the explanation: in the HNLF, the spectrum gets broadened due to the amplification of the noise floor based on the modulational instability that accompanies evolution of frequency combs. At the same time, there arise a Raman seed line at the remote distance of 43 THz that corresponds to the 3rd Raman band. When the seed achieves Raman threshold, it gives rise to the formation of a Raman soliton that is red-shifted due to self-frequency shift despite the impact of optical loss. The noise components between the frequency comb and the red-shifting Raman soliton are amplified to a supercontinuum with an almost equal spectral intensity. When only one monochromatic pulse is used as initial condition, a remote Raman seed is not observable. Also, the spectrum (that result through a cascade of self-shifted Raman solitons) is 200 nm less broad than in the case of a bi-chromatic two-laser input. Therefore, I conclude that the formation of a frequency comb (for which a bi-chromatic input is essential) is needed to induce a remote Raman seed that, in turn, allows to generate a 1000 nm supercontinuum suitable for infrared spectroscopy.

Further studies are needed to understand why the Raman seed arises at such a remote distance of 43 THz (3rd band) and not, for instance, at 13 THz which would coincide with the first Raman band. Also, an explanation of how the noise floor between the frequency comb and the remote Raman soliton is amplified has to be derived. It is to understand whether this noise amplification occurs only due to the impact of the modulational instability or whether the emission of dispersion waves that might go along with the Raman soliton formation contributes to the formation of the supercontinuum. The ultimate goal would be to generate a supercontinuum with a much broader range starting at wavelengths considerably below 1550 nm. For this, it has to be studied whether the Erbium amplifier is able to support this idea or it might be better to use other amplifying media such as Ytterbium- or Bismuth-doped fibers.

5. References

[1] B. H. Stuart, *Infrared Spectroscopy: Fundamentals and Applications*, Analytical Techniques in the Sciences (John Wiley & Sons, Ltd, 2004).

[2] J. R. Taylor, "Tutorial on fiber-based sources for biophotonic applications," J. Biomed. Opt. **21**, 061010 (2016).

[3] J. H. Lee, J. van Howe, C. Xu, and X. Liu, "Soliton Self-Frequency Shift: Experimental Demonstrations and Applications," IEEE J. Sel. Top. Quantum Electron. **14**, 713–723 (2008).

[4] G. P. Agrawal, "Introduction," in *Nonlinear Fiber Optics* (Academic Press, 2012), pp. 1–3.

[5] M. Zajnulina, J. M. C. Boggio, M. Böhm, A. A. Rieznik, T. Fremberg, R. Haynes, and M. M. Roth, "Generation of optical frequency combs via four-wave mixing processes for low- and medium-resolution astronomy," Appl. Phys. B **120**, 171–184 (2015).

[6] M. Zajnulina, M. Böhm, K. Blow, A. A. Rieznik, D. Giannone, R. Haynes, and M. M. Roth, "Soliton radiation beat analysis of optical pulses generated from two continuous-wave lasers," Chaos **25**, (2015).

[7] M. Zajnulina, M. Böhm, D. Bodenmüller, K. Blow, J. M. C. Boggio, A. A. Rieznik, and M. M. Roth, "Characteristics and stability of soliton crystals in optical fibres for the purpose of optical frequency comb generation," Opt. Commun. **393**, (2017).

[8] S. V. Chernikov, D. J. Richardson, D. N. Payne, and E. M. Dianov, "Soliton pulse compression in dispersion-decreasing fiber," Opt. Lett. **18**, 476 (1993).

[9] G. P. Agrawal, "Stimulated Raman Scattering," in *Nonlinear Fiber Optics*, 5th ed. (Academic Press, 2012), pp. 73–86.